Lithos 262 (2016) 606–619

Contents lists available at ScienceDirect

Lithos

journal homepage: www.elsevier.com/locate/lithos

Geochemical and mineralogical characteristics of the Yonghwa phoscorite–carbonatite complex, South Korea, and genetic implications

Jieun Seo [a,c], Seon–Gyu Choi [a,*], Jung–Woo Park [b], Scott Whattam [a], Dong Woo Kim [a], In–Chang Ryu [c], Chang Whan Oh [d]

[a] Department of Earth and Environmental Sciences, Korea University, Seoul 02841, South Korea
[b] School of Earth and Environmental Sciences & Research Institute of Oceanography, Seoul National University, Seoul 08826, South Korea
[c] Department of Geology, Kyungpook National University, Daegu 41566, South Korea
[d] Department of Earth and Environmental Sciences, Chonbuk National University, Jeonju 54896, South Korea

ARTICLE INFO

Article history:
Received 18 February 2016
Accepted 5 August 2016
Available online 16 August 2016

Keywords:
Phoscorite–carbonatite
Fenitization
Fe mineralization
Yonghwa
Korea

ABSTRACT

The Yonghwa phoscorite–carbonatite complex occurs as an isolated individual body with an inclined pipe shape within the Precambrian Gyeonggi Massif, South Korea. The phoscorite consists mainly of olivine, apatite, magnetite, carbonates, amphibole, and phlogopite, and can be subdivided into two types, olivine-rich and apatite-rich. The carbonatite is composed of calcite, Mg-rich dolomite, Fe-rich dolomite, magnetite, apatite, and/or siderite. Intensive fenitization occurred along the boundary between the complex and the wall rocks of leucocratic banded gneiss and garnet-bearing metabasite. The paragenetic sequences of the phoscorite–carbonatite complex demonstrate that the early crystallization of silicate minerals was followed by the crystallization of carbonates as the carbonatitic melt cooled. Magnetite occurs within the complex, and the carbonatites have Fe contents that are higher than typical ferrocarbonatites, due to the high magnetite contents. The rare earth elements (REEs) in the phoscorites and carbonatites are weakly fractionated and show enrichments of LREEs and Nb relative to HREEs. Furthermore, the apatites reflect the fractionated trends of LREEs relative to HREEs. Phoscorite apatites are enriched in Sr and show substitutions between Ca and Sr. Mica chemistry reflects the evolutionary trend of Fe^{2+} and Mg^{2+} in the phoscorite–carbonatite melt without Al substitution. Micas exhibit high values of Mg# in the phoscorite–carbonatite complex, but lower values in fenites. Via thermodynamic analysis, the early stability fields of magnetite–pyrrhotite–graphite–carbonate assemblages indicate that the Yonghwa phoscorite and carbonatite crystallized under conditions of 600 °C, 2 kbar, and $X_{CO2} = 0.2$. Afterward, melts underwent an evolution to the late stability fields of magnetite–pyrite–pyrrhotite–ilmenite assemblages. The $\delta^{13}C$ and $\delta^{18}O$ isotopic compositions of carbonates in the Yonghwa phoscorite–carbonatite complex are −8.2‰ to −3.4‰ and 6.6 to 11.0‰, respectively, and together with the sulfur isotope compositions of the sulfides ($\delta^{34}S$ values of about 0.2‰ to 2.2‰) indicate a primary mantle source of the magmas. Phlogopites from the fenites yielded K–Ar ages of 193.4 ± 4.9 and 195.0 ± 5.1 Ma, which demarcate the timing of the cooling of the phoscorite–carbonatite intrusion, and indicate that the phoscorite–carbonatite may be related to a post-collisional magmatic regime. The discovery of this complex marks the first known occurrence in Korea, of Fe and Nb–REE mineralization related to phoscorite–carbonatite igneous activity.

1. Introduction

On a global basis, carbonatites have been reported from about 500 localities, but phoscorite is a rarely reported rock type, having been identified from only 21 occurrences worldwide (Krasnova et al., 2004; Woolley, 2001). These rocks are important from both an economic and scientific point of view. Economically, they are not only major potential sources of iron but also rare earth elements, niobium, phosphorus, and thorium (Bambi et al., 2012; Barbosa et al., 2012; Melgarejo et al., 2012; Mitchell, 2015; Sharygin et al., 2009). From an academic point of view, the scarcity of these unique rock types means they are valuable in terms of providing unique information on the petrogenetic and tectonic environment in which they formed.

A phoscorite–carbonatite complex was recently discovered in the Yonghwa area, South Korea (Fig. 1; Choi et al., 2013). It occurs as an inclined elliptical pipe in which the phoscorite and carbonatite intermingled showing gradual transitions between the two rock types. Although carbonatites generally occur in association with alkaline series rocks, the Yonghwa phoscorite–carbonatite complex occurs as a small, discrete body without any associated alkaline rocks (Harmer, 1999;

* Corresponding author.
E-mail address: seongyu@korea.ac.kr (S.–G. Choi).

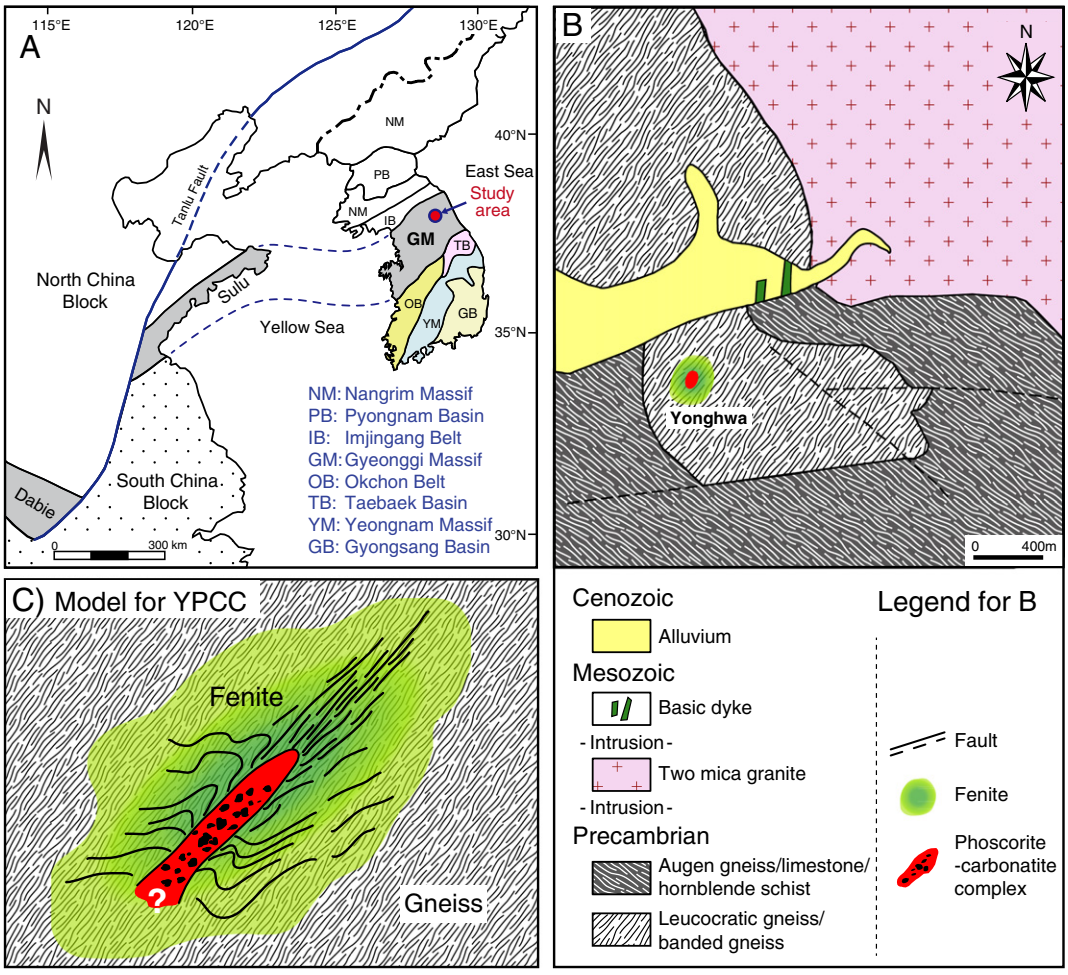

Fig. 1. (A) Simplified regional geological map of the Yonghwa area, South Korea. (B) Detailed geological map of the study area in A. (C) Schematic diagram of the Yonghwa phoscorite–carbonatite complex (YPCC) shown in B.

Morbidelli et al., 1995; Sharygin et al., 2011; Veksler et al., 1998; Woolley and Kjarsgaard, 2008). In this paper, we describe the petrological, mineralogical, and geochemical features of the Yonghwa phoscorite–carbonatite complex in order to constrain its petrogenesis, and to investigate the potential for its hosting an ore deposit. In addition, we analyzed carbon, oxygen, and sulfur isotopes in order to understand the origin of the phoscorite–carbonatite magma, and determined K–Ar ages in order to constrain the age of the complex. Our results have implications for the petrogenesis of carbonatites elsewhere.

2. General geology

Tectonostratigraphic units in Korea include the Proterozoic Gyeonggi Massif, the Neoproterozoic–Paleozoic Okcheon metamorphic belt, the Paleozoic Taebaeksan Basin, the Proterozoic Yeongnam Massif, and the Mesozoic Gyeongsang Basin (Fig. 1A). The southern segment of the Gyeonggi Massif has been interpreted recently as an extension of the Permo-Triassic Dabie–Sulu orogenic belt that lies between the North China and Yangtze blocks (Oh and Kusky, 2007; Oh et al., 2005, 2006; Seo et al., 2010). The Gyeonggi Massif is composed of leucocratic gneisses, banded biotite gneisses, quartzites, mica schists, marbles, and metabasites, and these rocks are intruded by Jurassic two-mica granite. The Yonghwa phoscorite–carbonatite complex was discovered recently in the leucocratic banded gneiss of the Gyeonggi Massif (Fig. 1B). Fenite occurs around the phoscorite–carbonatite intrusion. On the basis of drilling data, the phoscorite–carbonatite complex is a pipe-like shape that is inclined to the NE (Fig. 1C). Magnetite-rich ore bodies occur within the complex. Carbonatite veins are commonly observed in the phoscorite, carbonatite, fenite, and country rocks. The Yonghwa phoscorite–carbonatite and Fe–Nb ores were identified on the basis of the petrological and geochemical data that are available as Supplementary Table A.1.

3. Petrography

3.1. Phoscorite–carbonatite

The phoscorite–carbonatite series rocks are different from those usually associated with silicate magma (Heinrich, 1967). The rock series comprises various minerals including silicates, carbonates, phosphates (mainly apatite), and oxides (mainly magnetite and minor Nb-oxides), and even though these minerals show an irregular distribution, there is a continuous petrographic variation between phoscorite and carbonatite. The abundances of silicate and phosphate minerals decreases from the phoscorite to the carbonatite, while the percentage of carbonate minerals increases, and there are some relatively late-stage carbonatite veins (Fig. 2). The classic definition of carbonatite is a medium- to coarse-grained igneous rock that contains more than 50 modal% magmatic carbonate minerals and <20 wt% SiO_2 (Le Maitre, 2002). However, a recent and widely accepted definition is that carbonatite is composed of more than 30 vol% magmatic carbonate minerals, regardless of SiO_2 content (Mitchell, 2005). Here, we follow the definition of Mitchell (2005), so that rocks with <30 vol% carbonate

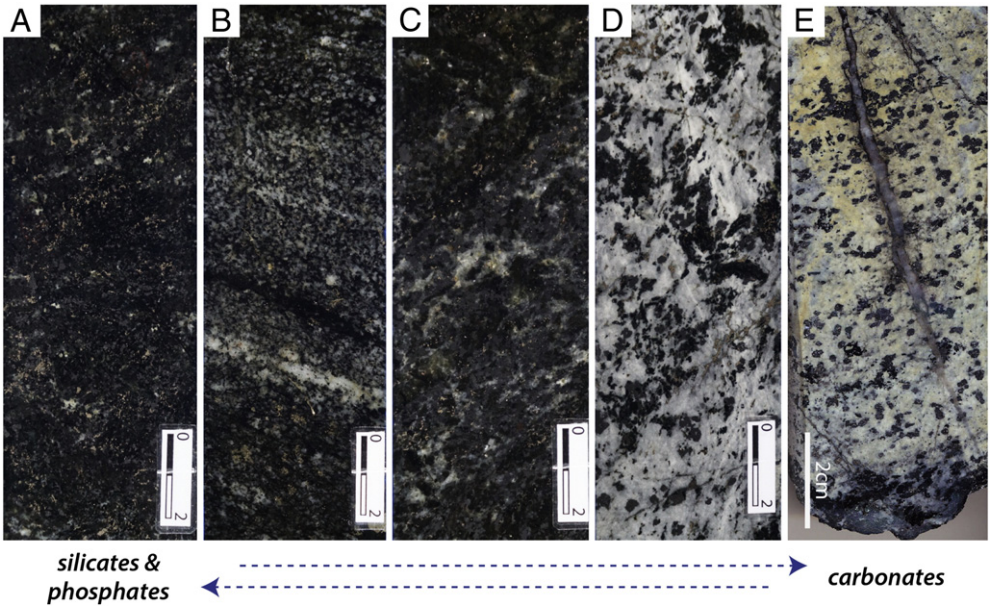

Fig. 2. Photographs of representative polished core specimens of phoscorite and carbonatite from the Yonghwa area. (A to E) The modal contents of silicates decrease and those of carbonates increase continuously from phoscorite to carbonatite.

minerals are phoscorite and rocks with >30 vol% are carbonatite. Commonly, phoscorite consists of magnetite, olivine, and apatite (Russell et al., 1954). The Yonghwa phoscorites are dark green and consist mainly of olivine, apatite, magnetite, phlogopite, dolomite, and clinohumite, with accessory pyrrhotite, monazite, uraninite, baddeleyite, columbite, and pyrochlore, and they can be subdivided into olivine-rich and apatite-rich varieties (Fig. 3A to F). The Yonghwa carbonatites are gray to light grayish white in colour, and composed mainly of calcite and various other carbonate minerals (e.g., Mg-rich dolomite, Fe-rich dolomite, siderite, magnesite, and strontianite), as well as magnetite, apatite, minor mica and olivine, and accessory graphite, ilmenite, pyrrhotite, and pyrite (Fig. 3G, H). The modal compositions of the Yonghwa phoscorites plot mainly within the field of phoscorite, as defined by Yegorov (1993), although some plot in the fields of olivine magnetitite, magnetite forsteritite, and apatite forsteritite (Fig. 4A), which makes them similar to the Kovdor phoscorites in Russia (Krasnova et al., 2004).

3.2. Fenite

Intensive fenitization caused by the intruding phoscorite–carbonatite magma occurred within a few meters of the boundary with the host leucocratic banded gneiss or garnet-bearing metabasite, and most of the original textures of the gneiss were removed or only partly remain. Some gneiss was gradually transformed to fenite by hydrothermal alteration (metasomatism). The fenites in the Yonghwa area are mainly composed of mica, amphibole, apatite, albite, pyrite, and ilmenite. The banded gneiss and metabasite were cut by multiple carbonate veins of various sizes during the process of alteration.

4. Analytical methods

Whole-rock major and trace element concentrations in the Yonghwa phoscorites and carbonatites were determined using inductively coupled plasma–atomic emission spectrometry (FUS–ICP–AES; Termo JarrelAsh ENVIRO II), inductively coupled plasma–mass spectrometry (FUS–ICP/MS; Perkin Elmer Optima 3000), and instrumental neutron activation analysis at Activation Laboratories Ltd., Canada. Representative whole-rock compositions of the Yonghwa rocks are available as Supplementary Table A.1.

Mineral compositions were determined using an electron microprobe (JEOL JXA-8600 SX) with energy dispersive spectroscopy (INCA-6025, Oxford Instruments) at Korea University, Seoul, South Korea. The microprobe was operated with an accelerating voltage of 15.0 kV, a beam current of 3.0 nA, a live time of 100 s, and a probe diameter of 3 μm. Analytical results are available as Supplementary Tables A.2–A.8.

Trace elements of the apatites were determined using laser ablation–inductively coupled plasma–mass spectrometry (LA–ICP–MS) at the Research School of Earth Science, Australian National University, Canberra, Australia. The system consisted of an excimer laser (λ = 193 nm, Compex 110, Lambda Physik) and a quadrupole ICP–MS (Agilent 7700×). The LA–ICP–MS analyses were performed using a laser pulse rate of 5 Hz, a spot size of 47 μm, and an energy of 2.5 J/cm^2. NIST 610 glass was used as a primary standard, and Ca obtained by the electron microprobe analysis was employed as an internal standard to correct the yield differences between the standard and the unknown samples. The trace element compositions of representative apatites are shown in Supplementary Table A.9.

Carbon and oxygen isotopic compositions were determined using a MAT235 mass spectrometer at the Chinese Academy of Sciences, Beijing, China. The carbon and oxygen standards employed were the Pee Dee Belemnite (PDB) and Standard Mean Ocean Water (SMOW), respectively. The analytical precision was better than ±0.2‰ for both $\delta^{13}C$ and $\delta^{18}O$. Isotopic compositions of the carbonatites are listed in Table 1.

The sulfur isotopes of pyrrhotite and pyrite were measured at Activation Laboratories Ltd., Canada. The $\delta^{34}S$ data given in Table 2 are reported relative to the Canyon Diablo Troilite (CDT).

The K concentrations were determined by ICP, and argon analyses were undertaken using the isotope dilution procedure on a noble gas mass spectrometer at Activation Laboratories Ltd., Canada.

5. Whole-rock chemistry of the phoscorite and carbonatite

The general subdivision of the carbonatites with SiO_2 < 20 wt% can be achieved using wt% oxides in CaO–MgO–(FeO* + MnO) space (Woolley and Kempe, 1989), and under this scheme the Yonghwa carbonatites are Mn-rich ferrocarbonatites with high proportions of magnetite (Fig. 4B). On the SiO_2 vs. CaO (wt%) and SiO_2 vs. MgO (wt%) binary diagrams of Peccerillo and Taylor (1976), the Yonghwa phoscorites

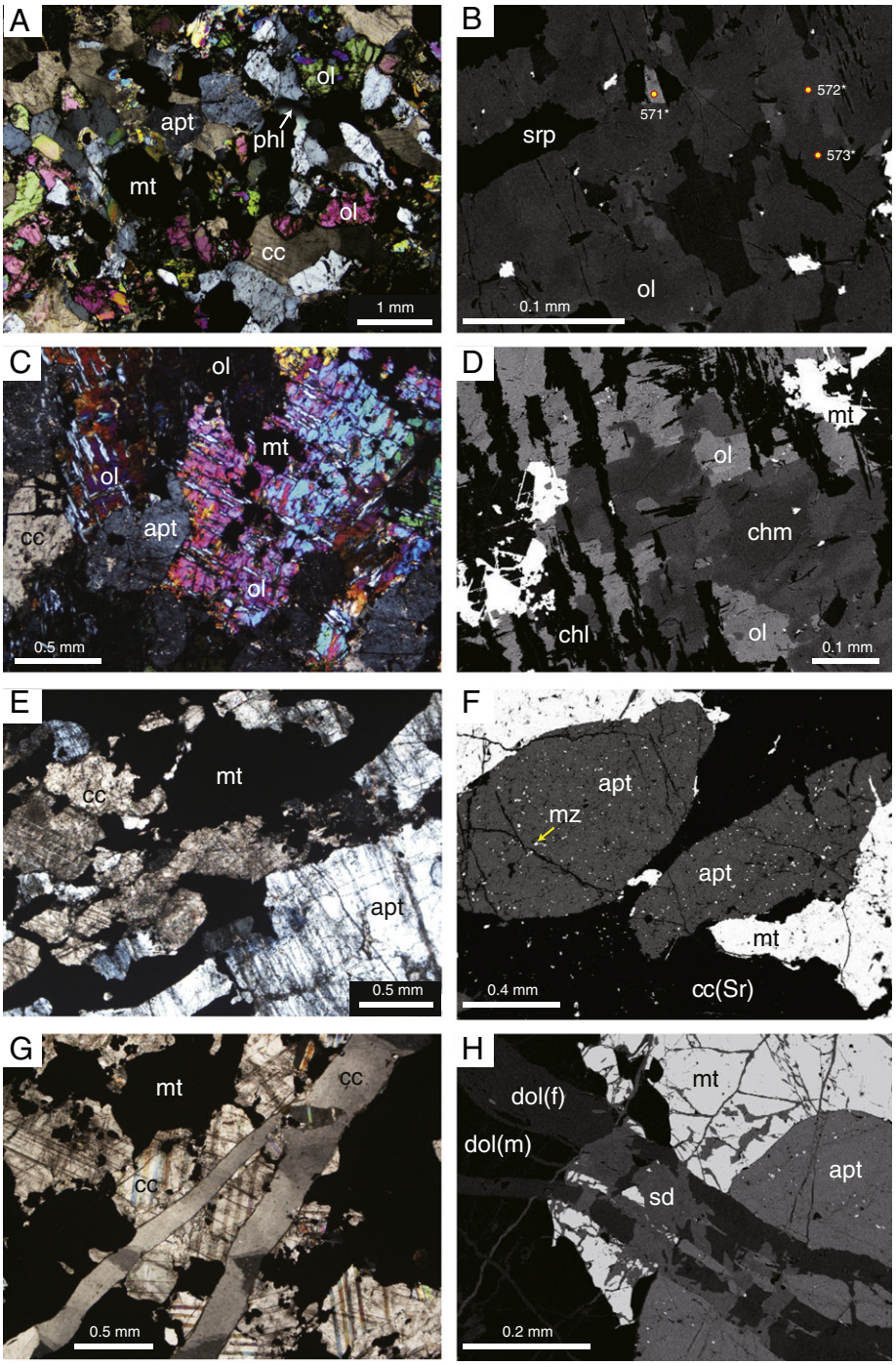

Fig. 3. Photomicrographs (cross polarized light) and backscattered electron (BSE) images of the phoscorite (A to F) and carbonatite (G to H) from the Yonghwa area. (A) Phoscorite showing olivine, magnetite, apatite, and carbonate assemblages. (B) BSE image of sample YH1102-7B. Numbers 571* to 573* refer to analytical points in bright and dark domains of olivine in sample YH1102-7B, respectively (Table 2). (C) Altered olivine showing lattice texture in sample YH1102-7B. (D) BSE image of the lattice textured olivine altered to clinohumite. Other alteration products are serpentine, magnetite, and chlorite. (E) Apatite-rich phoscorite mainly composed of apatite and magnetite. (F) BSE image of apatite-rich phoscorite. Numerous fine grained strontianite grains are present within the Sr-bearing calcite. (G) Carbonatite composed of carbonate minerals and magnetite, with late calcite crosscutting early calcite and magnetite. (H) BSE image of carbonatite. Various carbonate minerals showing cross cutting relationships. Abbreviations: apt = apatite; cc = calcite; chl = chlorite; chm = clinohumite; dol(m) = Mg-rich dolomite; dol(f) = Fe-rich dolomite; mt = magnetite; mz = monazite-(Ce); ol = olivine; phl = phlogopite; sd = siderite; and srp = serpentine.

and carbonatites are comparable with other typical phoscorites and carbonatites (Downes et al., 2005; Fig. 5A, B). The Yonghwa phoscorites contain 6.2–49.8 wt% SiO_2, 10.1–47.7 wt% $Fe_2O_3^{tot}$, 3.3–15.0 wt% MgO, and 5.3–18.6 wt% CaO, and have values of Mg# [= Mg / (Mg + Fe^{2+})] in the range of 13.7–28.5 (Table A.1). Compared with the Sokli phoscorite of Finland (Lee et al., 2004), the Yonghwa phoscorites are more enriched in P_2O_5 and MnO because they contain more apatite and Mn-rich olivine (up to 42.5 wt% MnO), but the TiO_2 contents are lower because of the rarity of ilmenite-group minerals. The carbonatites exhibit a wide compositional range, and some carbonatite samples are enriched in Si (approximately 14.0 wt% SiO_2), due to the presence of olivine and phlogopite. The phoscorites and carbonatites have relatively high contents of strontium (1037–9255 ppm and 1284 to >10,000 ppm, respectively) and niobium contents that vary from 138 to >1000 ppm in both rock types. The

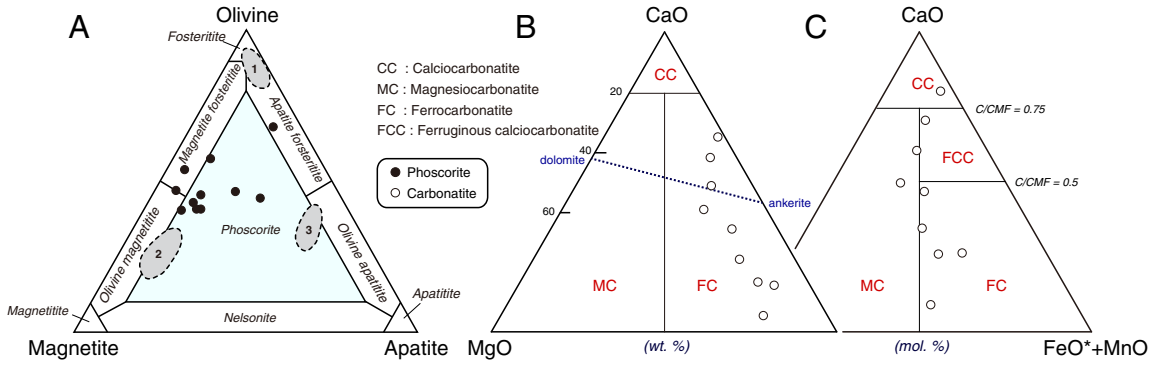

Fig. 4. (A) Classification of phoscorite by modal analysis. Classification scheme from Yegorov (1993). (B) Ternary plot of CaO–MgO–(FeO + MnO) showing classification of carbonatite with SiO_2 < 20 wt% (after Woolley and Kempe, 1989). (C) Ternary plot of CaO–MgO–(FeO + MnO) showing mole % classification of carbonatite after Gittins and Harmer (1997). 1 = Kovdor olivine-rich phoscorites; 2 = Kovdor magnetite-rich phoscorites; and 3 = Kovdor apatite-rich phoscorites (Kovdor fields from Krasnova et al., 2004).

high Sr and Nb contents in the phoscorites and carbonatites result from the presence of strontianite and Nb-oxides such as columbite and pyrochlore, respectively. Although the Yonghwa carbonatites have large variations in Fe content, and the maximum value is higher than that of average ferrocarbonatite (7.4 wt% $Fe_2O_3^{tot}$) according to the classification scheme of Woolley and Kempe (1989) (Fig. 4B). The Si contents are also higher than in the average ferrocarbonatite whereas Ti and REE concentrations are lower. The REE and trace element contents of the phoscorite and carbonatite were respectively normalized to CI-Chondrite and primitive mantle values (Sun and McDonough, 1989) in Fig. 5C and D. The La_N/Yb_N ratios for the phoscorites are 19–109, and those for the carbonatites are 35–110 (Table A.1). Chondrite-normalized REE distribution patterns for the Yonghwa phoscorites and carbonatites are similar to or less fractionated than in primitive phlogopite picrite. One carbonatite sample with a relatively minor amount of apatite also shows a similar pattern, despite the low REE contents. The phoscorites (total REEs = 488–3646 ppm) and most carbonatites (1031–4220 ppm) have relatively high total REE contents compared with the apatite-poor carbonatites (56 ppm; sample YH1105-4), and based on Eu/Eu^* [$=Eu_N/\sqrt{(Sm_N \times Gd_N)}$] values, the phoscorites (0.85–1.08) and carbonatites (0.94–1.08) do not show significant Eu anomalies (Table A.1; Fig. 5C). Primitive mantle normalized trace element patterns for the phoscorites and carbonatites show significant depletions in Rb, Ba, Th, and Zr, and relative concomitant enrichments in Nb, Sr, and LREEs (Fig. 5D). Extreme enrichment in Nb (138 up to 1000 ppm) and poor of Ta (0.10–5.34 ppm) with high Nb/Ta ratios are also characteristic of the Yonghwa phoscorite–carbonatite complex.

Table 1
Representative C–O isotope analyses of carbonates in the Yonghwa area, South Korea.

Sample	Mineral	Occurrence	$\delta^{13}C_{PDB}$ ‰	$\delta^{18}O_{V\text{-}SMOW}$ ‰
YH1104-8	Carbonates	Phoscorite	−7.6	9.4
YH1104-9	Carbonates	Phoscorite	−7.2	9.3
YH1102-11	Carbonates	Carbonatite	−7.3	9.2
YH1103-14A	Dolomite	Carbonatite	−8.2	9.6
YH1103-7	Carbonates	Carbonatite	−5.8	10.4
YH1104-4	Carbonates	Carbonatite	−6.7	7.7
YH1104-17	Carbonates	Carbonatite	−6.2	9.0
YH1103-9	Calcite	Vein in carbonatite	−6.0	6.9
YH1102-16	Calcite	Vein in fenite	−5.6	6.6
YH1103-25	Calcite	Vein in fenite	−4.3	7.1
YH1103-2	Calcite	Vein in gneiss	−4.0	7.2
YH1101-3	Carbonates	Vein in gneiss	−3.7	9.6
YH1101-10	Carbonates	Vein in gneiss	−4.8	11.0
YH1104-25	Carbonates	Vein in gneiss	−3.4	9.1
YH1103-22C	Calcite	Vein in garnet-bearing metabasite	−4.4	7.3
YH1104-24	Carbonates	Vein in garnet-bearing metabasite	−4.1	6.8

6. Mineral paragenesis and composition

6.1. Silicates

Olivine shows a variable range of composition in the Yonghwa phoscorite. It is commonly replaced by clinohumite, and altered to chlorite, serpentine, and magnetite. The primary olivine (type A) has mainly a granular texture, and it occurs with magnetite and apatite (Figs. 3A, 6A), while relatively late-stage olivine (type B) exhibits a mesh texture and is commonly altered to and/or replaced by clinohumite or occurs as relict olivine (Fig. 3B, C, D). Type A olivine contains 24.1–40.0 wt% MgO and 4.4–7.1 wt% MnO, and the values of Mg# are 0.56–0.79, whereas type B olivine has 11.1–29.5 wt% MgO, relatively high Mn contents of 7.5–42.5 wt% MnO, and values of Mg# in the range of 0.59–0.67 (Table A.2; Fig. 3B). In Mg–Fe–Mn space, Mn increases from the granular textured primary olivine to the lattice textured late-stage olivine (Fig. 7A). The Yonghwa phoscorite olivines exhibit high Mn contents (max. $Te_{0.56}$) relative to other phoscorite olivines from around the world.

Mica occurs in phoscorites, carbonatites, and fenites. However, because of the fenitization of the wall rocks, mica is dominantly concentrated in fenites. The textural features of micas in the Yonghwa phoscorites and carbonatites vary greatly between the rocks of different evolutionary stages. In the Yonghwa area, the micas can be divided into three types on the basis of colour and morphology. Type 1 is characterized by a blue tint and anhedral habit, although with unobvious cleavage in thin section (Fig. 6A, B), and this type usually occurs with apatite or olivine in the phoscorites. Type 2 is a greenish khaki colour and subhedral (Fig. 6C), and is accompanied by carbonates, suggesting that the latter represents a relatively late-stage mineral compared to the type 1 mica in the carbonatite. Type 3 mica, restricted to the fenite, is reddish brown to pale yellowish brown in colour, coarse-grained, and subhedral (Fig. 6D, E). The micas show large compositional variations in Fe and Mg from Mg-rich type 1 in the phoscorites to Fe-rich type 3 in the fenites (Fig. 7C). The phoscorite–carbonatite mica contains high BaO contents up to 2.1 wt% and is poor in TiO_2 while the fenite mica is

Table 2
Representative S isotope analyses of sulfides in the Yonghwa area, South Korea.

Sample	Mineral	$\delta^{34}S$ ‰
YH1106-10	Pyrrhotite	0.2
YH1103-17	Pyrrhotite	0.5
YH1105-7	Pyrrhotite	0.8
YH12-3-12	Pyrrhotite	2.1
YH1105-3	Pyrite	2.2

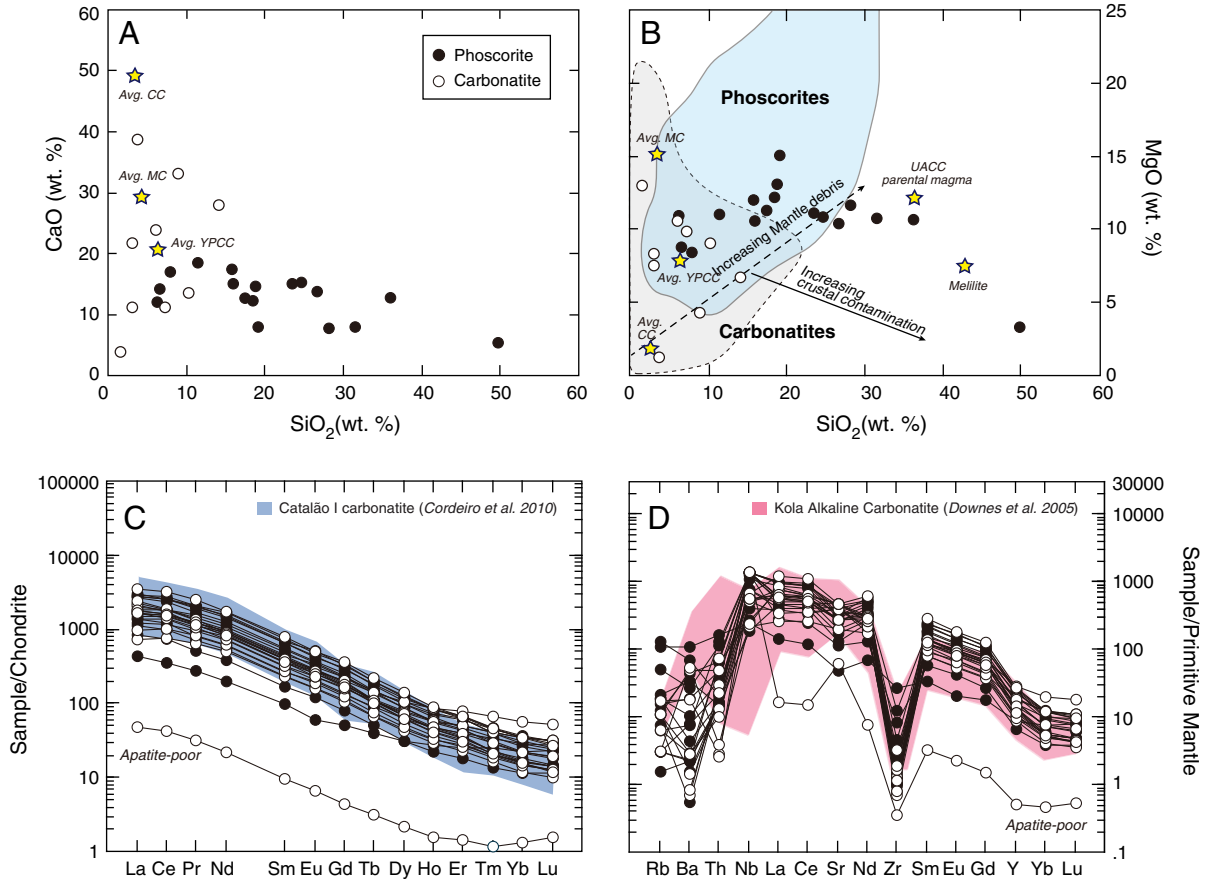

Fig. 5. Whole-rock major element compositions of phoscorite and carbonatite from the Yonghwa area. (A) SiO_2 vs. CaO diagram for Yonghwa phoscorite and carbonatite. (B) SiO_2 vs. MgO diagram for Yonghwa phoscorite and carbonatite. (C) Chondrite-normalized REE distribution patterns compared to Catalão I carbonatite (Cordeiro et al., 2010) and (D) primitive mantle-normalized trace element patterns compared to Kola alkaline carbonatite (Downes et al., 2005). Abbreviations: UACC = ultramafic alkaline carbonatite complexes. Phoscorite and carbonatite fields are from Downes et al. (2005) and Woolley and Church (2005).

characterized by relatively high TiO_2 contents of 0.5–1.8 wt% with BaO contents below the detection limit. Values of Mg# have ranges of 0.79–0.91, 0.61–0.87, and 0.37–0.62 in types 1, 2, and 3 micas, respectively (Table A.3). The compositions of the micas show an evolution from phlogopite to annite with increasing Fe (Fig. 7D). Micas in the phoscorite–carbonatite are Mg-rich phlogopites with substitution between Fe^{2+} and Mg^{2+} but without significant changes in Al^{3+} content, and this may simply reflect the evolutionary trend of the magma. In this regard, we note that the typical carbonatite micas in Brazil are tetra-ferriphlogopites (Brod et al., 2001) whereas the Yonghwa micas follow the "primary mica in silicate rocks" trend (Fig. 7D).

Amphiboles occur dominantly in the fenites in association with micas and as minor occurrences in the phoscorites and carbonatites (Fig. 6E). Amphiboles in the fenites are mostly calcium amphibole, whereas amphiboles in the carbonatite–phoscorite are sodium–calcium amphibole but with variable compositions (Fig. 7B). Amphiboles in fenites have Mg# values of 0.32–0.74 and 0.6–3.7 wt% Na_2O, whereas amphiboles in the phoscorites and carbonatites have relatively high values of Mg# (0.82–0.93 and 0.68–0.81, respectively) and contents of Na_2O (max. 5.4 wt%) (Table A.4).

6.2. Phosphates

Apatite is ubiquitous and the dominant phosphate mineral in all the rock types in the Yonghwa complex, making up 15–30 vol% of the phoscorites and carbonatites and 5–10 vol% of the fenites; it is particularly abundant in the olivine-poor phoscorites (Fig. 3E). Phoscorite and carbonatite apatite grains are subhedral to anhedral with fine-grained monazite inclusions. The grain boundaries between the apatites are commonly filled with late magnetite and carbonates (Fig. 3E, F). In contrast, apatite grains in the fenite occur mostly as anhedral round crystals without monazite inclusions, and some show compositional zoning (Fig. 6E). We analyzed the major and rare earth element concentrations in the apatites using EPMA (Table A.5) and LA–ICP–MS (Table A.9). The apatites are mostly fluorapatite with high contents of fluorine (b.d. ~ 4.1 wt%; avg. 2.5 wt%), and there are no clear differences among the compositions of apatites from the phoscorites, carbonatites, and fenites. The apatites contain 49.5–54.0 wt% CaO, 39.9–42.5 wt% P_2O_5, and 2.6–6.1 wt% SrO, and they show clear substitution trends between Ca^{2+} and Sr^{2+} with Sr/Ca ratios ranging from 1:2 to 1:1 (Fig. 8A). Phoscorite apatites are characterized by relatively high Mn and Sr contents (647–3760 and 16,683–35,546 ppm, respectively). Fenite apatites are characterized by relatively lower contents of Mn, but similar contents of Sr (237–848 and 12,491–30,952 ppm, respectively). When compared with those from other areas (e.g., NW Namibia; Drüppel et al., 2005), the Yonghwa phoscorite apatites show relatively high Mn and Sr contents, and the Yonghwa fenite apatites plot within the carbonatite field (Fig. 8B). Apatites from the fenites contain total REE contents of 1093 to 9385, whereas those from the phoscorites are appreciably richer in these elements (8181–40,742 ppm). REE distribution patterns for apatites from the phoscorites and fenites show differences in the amount of LREEs, although their concentrations of HREEs are similar (Fig. 8C, D).

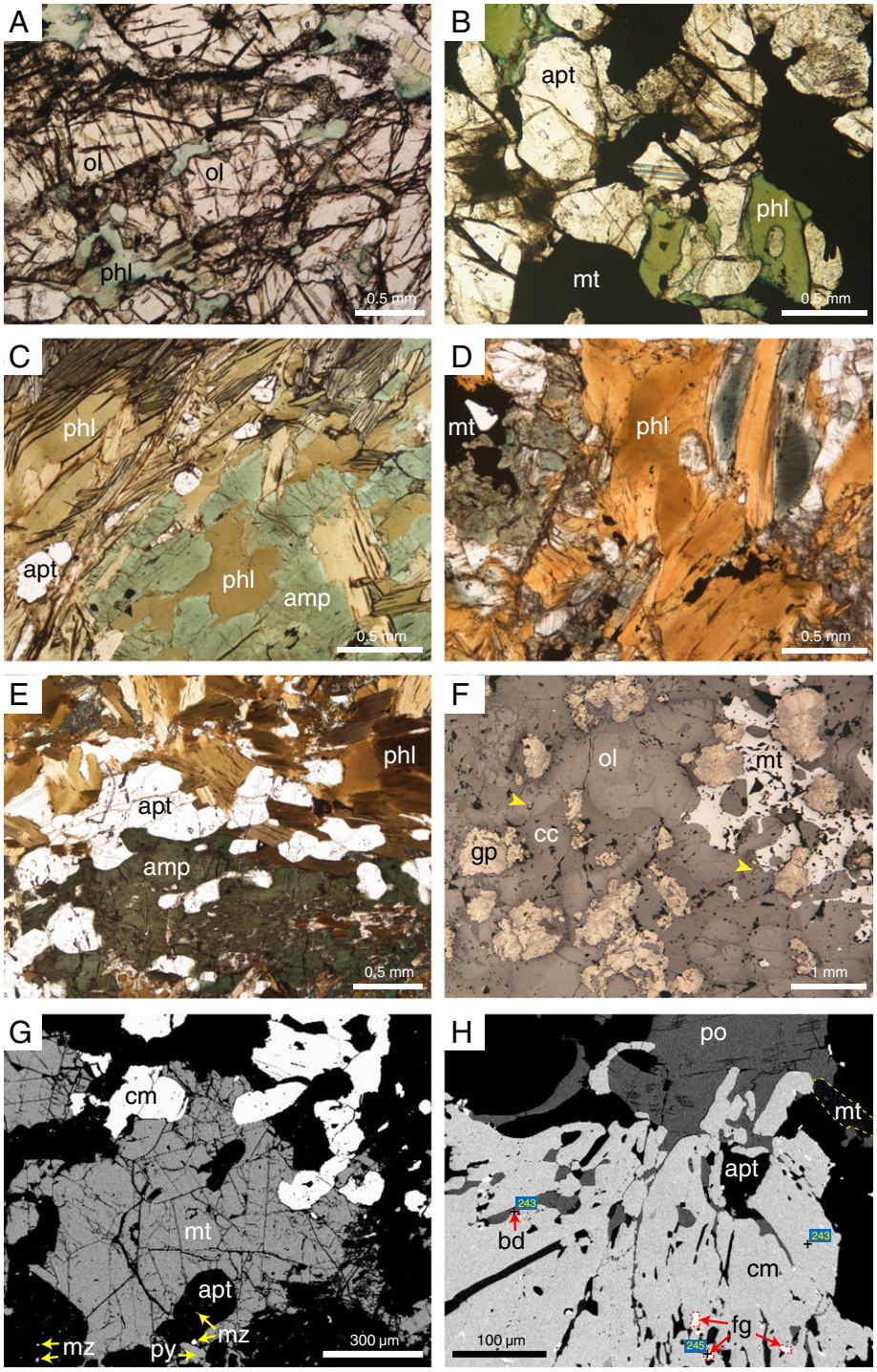

Fig. 6. Photomicrographs (plane polarized light, reflected light) and BSE images of some characteristic minerals from the Yonghwa complex. (A) Phlogopite in olivine-rich phoscorite showing a blue tint. (B) Phlogopite in the apatite-rich phoscorite is bluish green. (C) Phlogopite in the carbonatite is khaki green. (D, E) Phlogopite in the fenite exhibits a reddish to pale yellowish brown pleochroism. (F) Unaltered spherulitic graphite associated with primary olivine, apatite, carbonate, and magnetite. Some graphites occurs as inclusions within olivine or apatite (yellow arrow). Magnetite is an interstitial infilling between olivine and apatite. (G) Subhedral columbite and apatite with monazite inclusions surrounded by magnetite. (H) Graphic intergrowth between pyrrhotite and oxide minerals (magnetite, columbite). Abbreviations: bd = baddeleyite; cm = columbite; fg = fergusonite; fm = fersmite; po = pyrrhotite; and py = pyrite. (For interpretation of the references to color in this figure legend, the reader is referred to the web version of this article.)

Eu/Eu* and $(La/Yb)_N$ values for apatites from phoscorites are 0.92–1.03 and 61.4–444.9, respectively, and those values for apatites from the fenites are 0.61–1.11 and 5.6–160.9, respectively.

Monazite-(Ce) occurs in the form of inclusions within apatites from the Yonghwa phoscorites and carbonatite (Figs. 3F, 6G), and these monazites contain total REE contents of 60.5 to 69.3 wt%.

6.3. Oxides

Magnetite occurs mainly in the carbonatites and phoscorites, and rarely as disseminated grains in the fenites (Figs. 3, 6). It is anhedral and fills the spaces among the olivine, apatite, carbonates, and Nb-oxide minerals of the Yonghwa phoscorites and carbonatites (Figs. 3E,

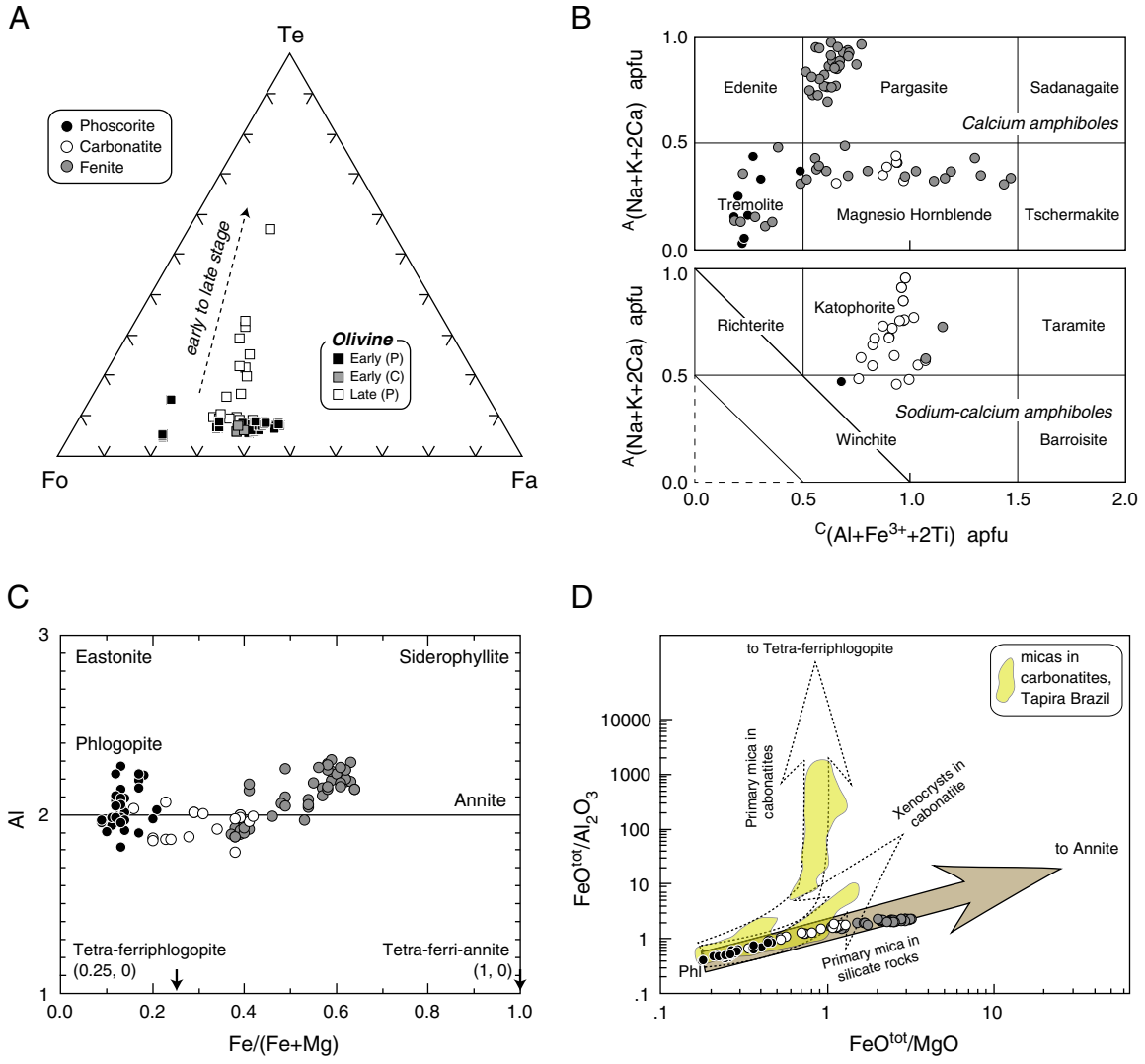

Fig. 7. Mineral compositions of the Yonghwa phoscorite–carbonatite and fenite. (A) Olivine compositions represent the increasing contents of Mn from an early to late stage. (B) $^{A}(Na + K + 2Ca)$ vs. $^{C}(Al + Fe^{3+} + 2Ti)$ content expressed in atoms per formula unit (apfu) in the A and C site of amphibole; amphibole groups outlined according to Hawthorne et al. (2012). (C) Variation of Al content (apfu) and Fe# [$= Fe^{2+} / (Mg + Fe^{2+})$] ratio in micas. (D) Iron variation with aluminum and magnesium within mica (Brod et al., 2001). The Yonghwa micas clearly plot along the phlogopite–annite trend and do not follow the trend of primary mica in carbonatites.

G, 6F, G). The Yonghwa magnetites are quite close to the Fe_3O_4 end-member composition with low contents of TiO_2 (avg. 0.5 wt%) and MnO (avg. 0.7 wt%).

Nb-oxide minerals occur mainly in the phoscorites and carbonatites. The Yonghwa phoscorites and carbonatites contain total REE concentrations of about 2000 ppm (Table A.1), and the high concentrations of REEs and Nb can be attributed to REE-oxides and phosphate minerals such as columbite, fersmite, fergusonite, pyrochlore, and apatite (Fig. 6G, H). Representative chemical data for the niobium-oxide minerals from the Yonghwa phoscorites and carbonatites are presented in Tables A.6 and A.7. The principal niobium minerals columbite ($FeNb_2O_6$) and fersmite ($CaNb_2O_6$) have very high contents of Nb_2O_5 (>75 wt%). The columbites contain 77.1–80.8 wt% Nb_2O_5, 7.4–12.3 wt% FeO, and 5.6–10.7 wt% MnO. Niobium cations (1.96–2.0 apfu) are preferentially retained within the B-site instead of Ta or Ti cations, and these columbites have high values of Mn# [$= (Mn / (Mn + Fe^{2+})$] in the range of 0.32–0.59. The fersmites contain 75.8–80.6 wt% Nb_2O_5 and 14.5–16.9 wt% CaO, and they are structured with the Nb cation (1.94–2.0 apfu) and Ca cation (0.88–1.0 apfu) in the B- and A-sites, respectively. The fergusonites have contents of Nb_2O_5 in the range of 42.0–56.6 wt% and high REE contents of 29.0–54.6 wt%. The pyrochlore group minerals from Yonghwa have high contents of Nb_2O_5 (41.9–66.7 wt%), ThO_2 (max. 33.9 wt%), UO_2 (max. 27.0 wt%), and LREEs (max. 20.3 wt%), and are Nb-abundant rather than Ti- or Ta-dominant in the Nb–Ti–Ta ternary compositional system. These chemical features are common to both the columbites and pyrochlores, and indicate an early stage of formation prior to substantial fractionation.

6.4. Carbonates, sulfides, and carbon minerals

Carbonate minerals occur mainly in the phoscorites and carbonatites, and the dominant types are Mg-rich dolomite, Fe-rich dolomite, and calcite, with subordinate strontianite, siderite, magnesite, and rhodochrosite. The relatively early carbonates are clear in thin section, while the relatively late carbonates are turbid. The clear carbonates are mainly Fe-rich or Mg-rich dolomite and the turbid carbonates are Mg-rich dolomite–calcite mixtures with small strontianite grains. The clear and turbid carbonates are intimately associated with one another. Sometimes the early Mg-rich dolomite is crosscut by Fe-rich dolomite or calcite (Fig. 3G, H). Mg-rich dolomites in the Yonghwa phoscorites and

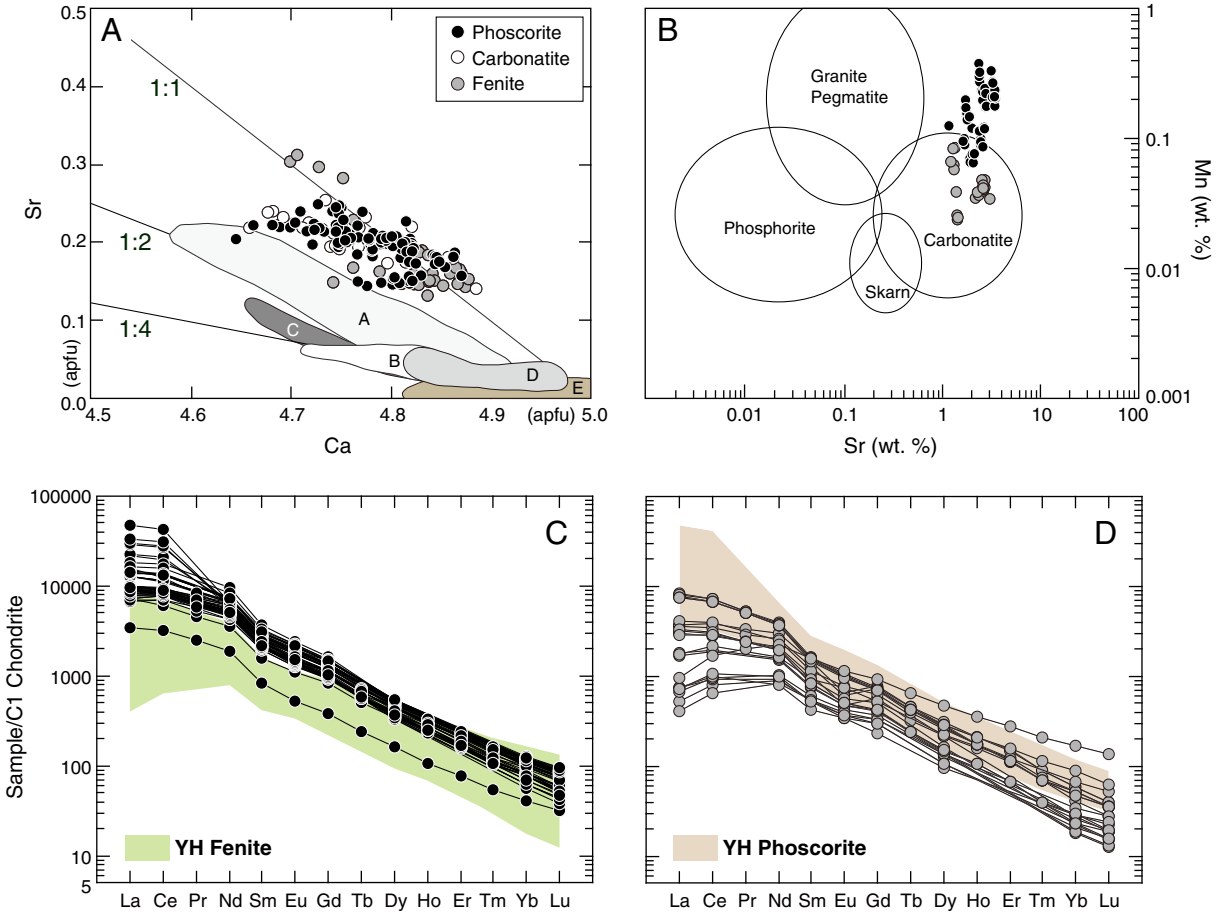

Fig. 8. Compositions of apatite in the Yonghwa phoscorite–carbonatite. (A) Variations in Ca and Sr contents (apfu). (B) Variations in Mn and Sr contents (wt%) compared with apatites in phoscorites, carbonatites, granite pegmatites, and skarns worldwide (Hogarth, 1989). (C) REE patterns of apatite in the Yonghwa phoscorite–carbonatite. (D) REE patterns of apatite in the Yonghwa fenite. A = nelsonite and B = phoscorite from Catalão, Brazil (Cordeiro et al., 2010); C = phoscorite–carbonatite, Sokli, Finland (Lee et al., 2004); D = phoscorite–carbonatite, Vuoriyarvi, Karelia (Karchevsky and Moutte, 2004); E = phoscorites, Kovdor, Russia (Krasnova et al., 2004); YH refers to Yonghwa.

carbonatites contain 13.4–18.7 MgO wt%, 1.7–6.4 FeO wt%, the Fe-rich dolomites contain 10.5–13.8 MgO wt%, 9.3–12.6 wt% FeO, and 1.9–3.6 wt% MnO, and the calcites contain an average of 49.7 CaO wt%, and 2.6 SrO wt% (Table A.8).

Sulfide minerals are observed as minor phases in the phoscorites and carbonatites as well as the associated fenite. Pyrrhotite was an early-crystallizing mineral that occurs mainly in association with minor chalcopyrite and sphalerite, whereas pyrite and marcasite formed at a relatively late stage.

Spherulitic graphite also occurs in the phoscorites and carbonatites in isolation or in aggregates with primary olivine, apatite, carbonate, and magnetite (Fig. 6F). The graphite occurs occasionally as inclusions within olivine or apatite.

7. Stable isotope geochemistry and geochronology

7.1. Carbon, oxygen, and sulfur isotopes

The $\delta^{13}C_{VPDB}$ values of the dolomites and calcites from the carbonatites and phoscorites range from −8.2‰ to −5.8‰, and the $\delta^{18}O_{VSMOW}$ values range from 6.9‰ to 10.4‰ (Table 1, Fig. 9). The $\delta^{13}C_{VPDB}$ values of dolomites and calcites from veins within the wall rocks show a relative enrichment in heavy carbon (−5.6‰ to −3.4‰), but similar $\delta^{18}O_{VSMOW}$ values (6.6‰ to 11.0‰; Table 1, Fig. 9). Carbonate minerals from the carbonatite–phoscorite complex, including the vein carbonatites, exhibit $\delta^{13}C$ and $\delta^{18}O$ values that generally fall in the field of primary, mantle-derived carbonatite. The pyrrhotites and pyrites in the Yonghwa deposit show a narrow range of sulfur isotope values ($\delta^{34}S_{CDT}$) from 0.2‰ to 2.2‰ (Table 2; Fig. 10), and these values are indicative of a primary mantle source.

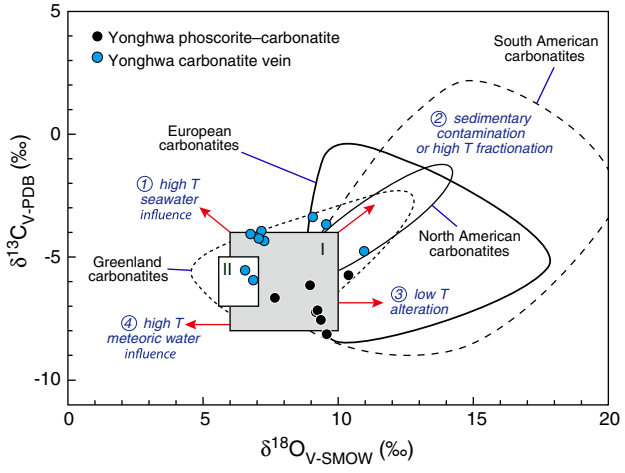

Fig. 9. Carbon ($\delta^{13}C_{V\text{-}PDB}$) vs. oxygen ($\delta^{18}O_{V\text{-}SMOW}$) isotopic variations in the carbonate minerals from the Yonghwa complex. I = primary igneous carbonate field (Taylor et al., 1967), II = primary mantle carbonatite (Keller and Hoefs, 1995). Other carbonatite fields are from Bell (2005). Arrows refer to the main processes affecting carbonatite isotope compositions (Deines, 1989; Demény et al., 1998).

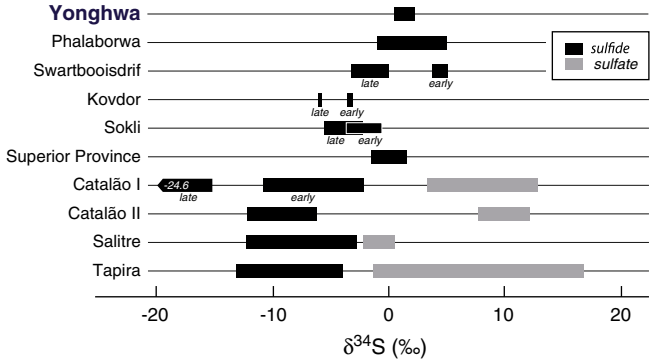

Fig. 10. $\delta^{34}S_{CDT}$ values for sulfide minerals in the Yonghwa phoscorite–carbonatite complex. Other data sources are: Phalaborwa, Africa (Hoefs et al., 1968; Mitchell and Krouse, 1975; von Gehlen, 1967); Sokli, Finland (Mäkelä and Vartiainen, 1978); Kovdor, Russia (Bell et al., 2015); Swartbooisdrif, Namibia (Drüppel et al., 2006); Superior Province, Canada (Farrell et al., 2010); central Brazil (Gomide et al., 2013).

7.2. K–Ar age dating

K–Ar dating of two phlogopite samples from fenites with 4.7 and 5.3 wt% potassium yielded ages of 195.0 ± 5.1 and 193.4 ± 4.9 Ma, respectively.

8. Discussion

8.1. Petrogenetic environment of Fe–Nb mineralization in the Yonghwa phoscorite–carbonatite complex

Our mineralogical study of the Yonghwa phoscorite–carbonatite complex shows that olivine, apatite, phlogopite, and graphite were the early crystallizing mineral assemblage, and that magnetite and carbonate crystallized predominantly in the late stage of magma differentiation (Fig. 11). During the late stage, the carbonatites typically lacked olivine and were enriched in magnetite and carbonate minerals. The Nb and REE-bearing minerals (columbite, fersmite, and pyrochlore) crystallized before the onset of magnetite crystallization. The compositional variations of micas and carbonate minerals seem to reflect compositional variations in the parental magma. The transition from calcite and Mg-rich dolomite to Fe-rich dolomite and siderite, as well as the trend from Mg-rich phlogopite (type 1) to Fe-rich phlogopite (type 2), suggests progressive iron enrichment in the relatively evolved magma that had undergone fractional crystallization. The increase in Sr with decreasing Ca from the early to the late apatites indicates that Sr was enriched during magma differentiation (e.g., Karchevsky and Moutte, 2004). In the post-magmatic hydrothermal stage, the carbonatites were cut by veins or veinlets of carbonate and quartz. The emplacement of these veins caused fenitization in the country rock with the crystallization of abundant phlogopite and amphibole.

The paragenetic sequence of magmatic sulfides, oxides, and carbonate minerals involved the assemblage magnetite–pyrrhotite–chalcopyrite–sphalerite–galena–columbite–graphite–carbonate at an early stage (Fig. 12), and some of the magnetite grains exhibit ilmenite exsolution. In contrast, late-stage magnetite crystallized in association with abundant pyrite. Elsewhere, Ryabchikov et al. (2008) suggested the graphite-bearing carbonatites of the Ukraine formed at 600 °C and 2 kbar on the basis of the mineral assemblages and the estimated depth of erosion, and Verwoerd (1966) estimated the barite-free carbonatite in Phalaborwa to have formed at around 675 °C, using the calcite–dolomite solvus geothermometer. Therefore, we used a Fe–Pb–Ti–C–O–H system at a temperature of 600 °C, a pressure of 2 kbar, and with $X_{CO2} = 0.2$ to analyze quantitatively the chemical parameters during the evolution of the Yonghwa phoscorite–carbonatite magma. In that system, a close paragenetic relationship among magnetite, pyrrhotite, graphite, chalcopyrite, and galena indicates a stability field between graphite and CO_2 below the QFM buffer. Carbonate mineral reactions intersect the magnetite–pyrrhotite reaction at $\log fH_2S = 0.1$ within the stability field of galena (Gieré, 1996), which is consistent with the occurrence of ilmenite in the Yonghwa rocks. In the final stage of evolution it was mainly carbonates that were produced under a post-magmatic hydrothermal environment, with the pyrite–magnetite assemblage confined to the carbonate veins and veinlets (Fig. 12).

8.2. Comparing the of genetic characteristics of the Yonghwa phoscorite–carbonatite with other phoscorite–carbonatite complexes

Worldwide, phoscorite–carbonatite complexes have been emplaced at depths that range from deep-seated intrusions to extrusive bodies,

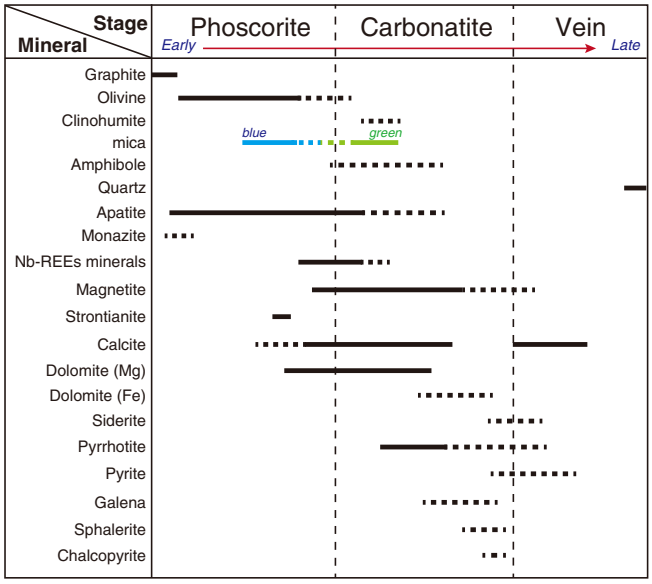

Fig. 11. Paragenetic sequence of the Yonghwa phoscorite–carbonatite complex.

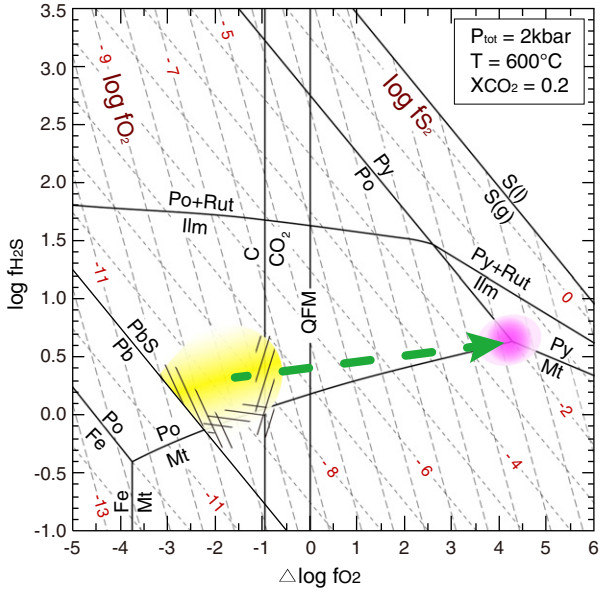

Fig. 12. Fe–Pb–Ti–C–O–H phase equilibrium diagram for the Yonghwa phoscorites and carbonatites ($P^{tot} = 2$ kbar, T = 600 °C, $X_{CO2} = 0.2$). Abbreviations: QFM = quartz–fayalite–magnetite buffer; Ilm = ilmenite; and Rut = rutile.

but most form isolated individual complexes that are made up of dykes, sills, pipes, or plugs (Le Maitre, 2002; Ribeiro et al., 2005). Most carbonatite complexes are composed dominantly of Ca- and Mg-rich carbonatites (Drüppel et al., 2005), and ferrocarbonatites are usually considered to represent the final products of fractional crystallization of the Ca–Mg carbonatite magma (Cooper and Reid, 1998; Drüppel et al., 2005; Gittins, 1989; Le Bas, 1977, 1999; Woolley and Kempe, 1989). Most extrusive carbonatites are closely associated with alkali magmatism (Krasnova et al., 2004; Woolley and Kjarsgaard, 2008). However, in the case of the Yonghwa carbonatites, the dominant rock-type is ferrocarbonatite, and it is the early product of fractional crystallization with enrichments in Fe, Mn, Sr, Ba, REEs, Th, and U. There is an absence of alkali magmatism. In the Yonghwa phoscorites, and to a lesser extent the carbonatites, the rocks are characterized by high Mn contents, as reflected in the compositions of olivine and apatite (Figs. 7A, 8B). The chondrite-normalized REE patterns and Nb/Ta ratios of the Yonghwa phoscorites and carbonatites indicate a parental magma that had not experienced significant fractionation, and which was probably close to the primary mantle-derived carbonatite magma. The Nb/Ta ratios of the Yonghwa phoscorites and carbonatites are extremely high in comparison with the average Nb/Ta ratios in phoscorites and carbonatites elsewhere (17 and 35, respectively; Chakhmouradian, 2006) or in primitive mantle (18; McDonough and Sun, 1995). The crystallization of magnetite and apatite is typical elsewhere of early stage carbonatites, and commonly accompanied by Nb minerals such as pyrochlore or columbite (Hogarth, 1989; Mariano, 1989; Mitchell, 2015). At Yonghwa, the pyrochlore group minerals have high contents of Nb_2O_5, ThO_2, UO_2, and LREEs, and are Nb-abundant rather than Ti- or Ta-dominant in the Nb–Ti–Ta space (apfu), and the high Nb/Ta ratios in the whole rock, pyrochlore, and columbite support a less fractionated primitive mantle-derived carbonatite magma. Therefore, on the basis of mineralogical, petrological, geochemical, isotopic data, and Nb/Ta ratios, we interpret the Fe-rich Yonghwa phoscorite–carbonatite complex inherently to be the product of a primitive parental magma rather than the product of a highly fractionated magma.

Silicate wall rocks intruded by phoscorite–carbonatites typically undergo fenitization (Drüppel et al., 2005; Heinrich, 1967; Le Bas, 2008; Lee et al., 2003; Platt and Woolley, 1990; Sharygin et al., 2011). Fenitization is the process of alkali metasomatism associated with alkaline igneous activity, including carbonatite intrusions, during which process the magma loses alkalis, which move into the wall rock during the early stages of fractionation of the carbonatite magma (Kresten, 1988; Le Bas, 2008). The fenitization of the wall rocks around carbonatites is usually strongly potassic and occurs with the production of K-feldspar (Dixey et al., 1935), but in cases where the carbonatite magma intrudes mafic rocks, the fenites are phlogopite- rather than feldspar-rich (Gittins et al., 1975). In the Yonghwa area, the fenites are composed mainly of mica, amphibole, apatite, and various accessory minerals, and feldspars are lacking, indicating that the fenites probably developed from a metabasic wall rock.

The redox condition of a magma can be traced through its mineralogy. For example, the phlogopites from carbonatites related to alkali complexes are commonly reported to be tetra-ferrimica, which shows a substitution between Al^{3+} and Fe^{3+} in the tetrahedral site (Brod et al., 2001; Lee et al., 2003). Moreover, in most cases, carbonatites preserve evidence of formation under high fO_2 (e.g., Arima and Edgar, 1981; Brigatti et al., 1996; Heathcote and McCormick, 1989). A typical result of such a high fO_2 environment is the tetra-ferriphlogopite in a carbonatite from Brazil (Brod et al., 2001). On the other hand, the Yonghwa micas follow the "primary mica in silicate rocks" trend (Fig. 7D), following the Fe^{2+}/Mg^{2+} trend of the silicate magma, and without substitution between Al^{3+} and Fe^{3+} in the tetrahedral site. In addition, many examples of spherulitic graphite are found within the Yonghwa phoscorites and carbonatites (Fig. 6F). These observations seem, therefore, to indicate that the Yonghwa phoscorite–carbonatite magmas were formed in a reduced state during cooling, and in the absence of alkali magmatism.

8.3. Origin of the Yonghwa phoscorite–carbonatite magma

Carbonatite is an igneous rock composed mainly of carbonate minerals that formed from a carbonate-rich magma (Bell, 1989; Faure, 2001; Heinrich, 1966). The production of a carbonatite magma is usually ascribed to low degrees of partial melting of metasomatized lithospheric mantle with high concentrations of Sr, Nb, and REEs (Bell and Simonetti, 2010; Faure and Mensing, 2005). Considering mantle heterogeneity, the initial $\delta^{13}C$ and $\delta^{18}O$ values of primary igneous carbonatites are in the ranges −5.1‰ to −7.3‰ and 6.0‰ to 10.0‰, respectively (Taylor et al., 1967; Fig. 9). High $\delta^{18}O$ values are due to contamination by country rock or hydrothermal processes (Demény et al., 1998; Santos and Clayton, 1995). The $\delta^{13}C$ and $\delta^{18}O$ values of carbonate minerals for the Yonghwa phoscorites, carbonatites, and vein carbonatites generally fall in the field of primary igneous and mantle-derived carbonatites, although the vein carbonatites show slightly higher $\delta^{13}C_{PDB}$ values (−5.6‰ to −3.4‰; Table 1). Thus the carbon and oxygen isotopic compositions of the Yonghwa phoscorites and carbonatites indicate they are igneous carbonatites that have not been subjected to secondary alteration processes (Deines, 1989; Nelson et al., 1988; Santos and Clayton, 1995; Taylor et al., 1967).

The mantle-derived sulfur isotopic values associated with mafic and ultramafic rocks of the asthenosphere are around 0.0 ± 2.0‰ (Nielsen, 1979; Ripley, 1999), and +0.5‰ for primitive upper mantle (Rollinson, 1993; von Gehlen, 1992). The $\delta^{34}S_{CDT}$ values of the Yonghwa sulfide minerals fall close to the accepted mantle range (−3‰ to +1‰: Ohmoto and Rye, 1979). Commonly the variations in S isotopic compositions are controlled by temperature, fO_2, and pH during melt generation and emplacement (Mitchell and Krouse, 1975; Ohmoto, 1972; Sakai, 1968). Even though shifts in the sulfur isotope values can occur due to several factors, such as those listed above, the sulfur isotope values of the Yonghwa phoscorites and carbonatites show a narrow range (0.2‰ to 2.2‰) typical of a magmatic origin, and consistent with the evidence of the carbon and oxygen isotope compositions. Moreover, the sulfur isotopic compositions are characteristic of magmatic sulfide mineral that have not been contaminated by crustal sulfate. The dominance of pyrrhotite in the sulfide minerals of the Yonghwa complex indicates high temperature conditions of 500–700 °C and more reduced conditions (e.g., Kovdor, Sayan; Mitchell and Krouse, 1975). The dominance of pyrrhotite and the presence of graphite indicate that the Yonghwa phoscorite–carbonatite magma maintained relatively high temperatures under reduced conditions during solidification of the magma. In summary, therefore, the data indicate that the Yonghwa phoscorite–carbonatite magma was derived from the mantle, and that the magma crystallized at high temperatures and under reduced conditions.

8.4. Tectonic significance of the Yonghwa phoscorite–carbonatite magmatism

Although carbonatites typically occur in anorogenic extensional tectonic settings, such as an intracontinental rift environment, carbonatites have also been reported from several collision-related orogenic settings (Bell et al., 1982; Chakhmouradian et al., 2008; Hou et al., 2006; Tilton et al., 1998). On the basis of geochemistry and trace element signatures, Chakhmouradian (2009) suggested there are two major types of continental carbonatite associated with alkali silicate rocks. Carbonatites emplaced in post-collisional tectonic settings are K-rich and associated with silica-saturated to undersaturated syenites, whereas carbonatites emplaced in rift-related environments are Na-rich and associated with silica-undersaturated syenites. In the Yonghwa complex, post-collisional phoscorite–carbonatite is not accompanied by alkali rock, although K-metasomatism (fenitization) has occurred around the phoscorite–carbonatite intrusion. Post-collisional magmatism is a

common feature of many collision belts around the world (Dewey, 1988). Recently, it has been proposed that the Hongseong–Odaesan belt is the extension of the Dabie–Sulu continental collision belt (located between the North and South China blocks), based on the occurrence of eclogite and mangerite (post-collisional granitoids) in the Hongseong and Odaesan areas, respectively (Oh and Kusky, 2007; Oh et al., 2005). Subsequently, Triassic post-collisional magmatism has been identified regionally in the northern Gyeonggi Massif to the north of the Hongseong–Odaesan collision belt by Seo et al. (2010), Choi et al. (2009), Williams et al. (2009), Jeong et al. (2008), Kim et al. (2011) and Sagong and Kwon (2005). These researchers have reported the following Triassic ages for the post-collisional magmatism in the northern Gyeonggi Massif: the Gwangcheon mangerite (232 ± 3 Ma, U–Pb SHRIMP zircon), the Haemi granite (233 ± 2 Ma, U–Pb SHRIMP zircon), the Namyang biotite granite (227 ± 3 Ma, U–Pb sphene), the Odaesan mangerite (229 ± 1 Ma, ID–TIMS: Isotope Dilution–Thermal Ionization Mass Spectrometry), the Odaesan monzodiorite (227 ± 2 Ma, U–Pb SHRIMP zircon), the Hongcheon hornblende biotite granodiorite (212 ± 27 Ma, Rb–Sr whole rock), the Jeongamri hornblende biotite granodiorite (227 ± 2 Ma, U–Pb sphene), and the Yangpyeong gabbro and monzonite (231 ± 3 Ma, U–Pb SHRIMP zircon). Carbonatites occur only in two locations on the Korean Peninsula, at Yonghwa and Hongcheon in the northern Gyeonggi Massif. The Hongcheon carbonatite is approximately 25 km away from the Yonghwa phoscorite–carbonatite complex. Recently, the intrusive age of the Hongcheon carbonatite was reported to be 227 ± 8 Ma (U–Pb SHRIMP monazite; Kim et al., 2016), implying that this carbonatite is also a product of the Triassic post-collision igneous activity. The K–Ar phlogopite ages of the Yonghwa fenite are 193–195 Ma, and therefore younger than the age of the Hongcheon carbonatite. However, the actual timing of intrusion of the phoscorite–carbonatite complex might be older than suggested by the K–Ar ages because the low closure temperature of the K–Ar system, which means the ages may represent a time during the cooling of the phoscorite–carbonatite magma; it is also possible that the ages were disturbed or reset during later Jurassic magmatism. We suggest, therefore, that the Yonghwa phoscorite–carbonatite may also be regarded as post-collisional, especially in view of its similar genetic origin to the nearby Hongcheon carbonatite. Contemporaneously with the Triassic post-collisional igneous activities (including the intrusion of phoscorite–carbonatites in the Korean Peninsula), the Shidao syenite complex in the Sulu belt and a swarm of carbonatite dykes in the Lesser Qinling orogen were emplaced along the southern margin of the North China Block after the collision of the North and South China blocks at around 220–240 Ma (e.g., Chen et al., 2003; Guo et al., 2006; Peng et al., 2008; Xu et al., 2011; Yang et al., 2005). These various lines of evidence indicate that the northern Gyeonggi Massif, located to the north of the Hongseong–Odaesan belt, can be regarded as the southern margin of the North China Block where Triassic post-collisional igneous activity occurred after the collision of the North and South China blocks.

9. Conclusions

The Yonghwa igneous intrusion shows a progression from phoscorite to carbonatite. The two rock types are closely related in terms of mineralogy and geochemistry, and their contacts are gradual suggesting a strong genetic link between the two rock types. The Yonghwa complex was intruded into a leucocratic banded gneiss and garnet-bearing metabasite, and these rocks were fenitized around the contact. During emplacement, silicate minerals (olivine and phlogopite) and apatite formed first, and subsequently the carbonate melts cooled to produce magnetite, sulfides, and carbonates such as strontianite, calcite, Mg-rich dolomite, Fe-rich dolomite, and siderite. Thermodynamic analysis of the early magnetite–pyrrhotite–graphite–carbonate assemblages indicates that the Yonghwa phoscorite and carbonatite crystallized under conditions of 600 °C, 2 kbars, and $X_{CO2} = 0.2$. The graphite–carbonate equilibrium intersects the magnetite–pyrrhotite reaction at log $f_{H2S} = 0.1$ within the stability field of PbS, and the presence of graphite indicates low fO_2. The $\delta^{13}C_{V\text{-}PDB}$ (−8.2‰ to −3.4‰) and $\delta^{18}O_{V\text{-}SMOW}$ (6.6‰–11.0‰) isotope compositions of calcite and dolomite from the carbonatites and the $\delta^{34}S_{CDT}$ (0.2‰–2.2‰) isotope values of the pyrrhotite and pyrite suggest a magmatic mantle origin for the phoscorite–carbonatite intrusion. K–Ar age dating of phlogopite from the Yonghwa fenite yielded dates of 193–195 Ma, but we suggest this date has been reset or disturbed, possibly during Jurassic magmatism, and that the Yonghwa complex was emplaced in the Triassic. This paper reports the first occurrence of Fe and Nb–REE mineralization associated with a phoscorite–carbonatite that is related to Triassic post-collisional magmatism on the Korean Peninsula.

Supplementary data to this article can be found online at http://dx.doi.org/10.1016/j.lithos.2016.08.006.

Acknowledgements

This work was supported by the Korea Institute of Energy Technology Evaluation and Planning (KETEP) grant funded by the Korea government Ministry of Knowledge Economy (20152510101890) and Basic Science Research Program through the National Research Foundation of Korea (NRF) funded by the Ministry of Science, ICT and Future Planning (2012R1A1A2005723). We are deeply indebted to A.R. Chakhmouradian and anonymous reviewer for their helpful comments. And, our thanks also go to A.C. Kerr for his editorial handling and comments of the manuscript.

References

Arima, M., Edgar, A.D., 1981. Substitution mechanisms and solubility of titanium in phlogopites from rocks of probable mantle origin. Contributions to Mineralogy and Petrology 77, 288–295.

Bambi, A.C.J.M., Costanzo, A., Goncalves, A.O., Melgarejo, J.C., 2012. Tracing the chemical evolution of primary pyrochlore from plutonic to volcanic carbonatites: the role of fluorine. Mineralogical Magazine 76, 377–392.

Barbosa, E.S.R., Brod, J.A., Junqueira–Brod, T.C., Dantas, E.L., Cordeiro, P.F.O., Gomide, C.S., 2012. Bebedourite from its type area (Salitre I complex): a key petrogenetic series in the late–cretaceous alto Paranaíba kamafugite–carbonatite–phoscorite association, Central Brazil. Lithos 144–145, 223–237.

Bell, K. (Ed.), 1989. Carbonatites: Genesis and Evolution. Unwin Hyman, London.

Bell, K., 2005. Carbonatites. In: Selley, R.C., Cocks, L.R.M., Plimer, I.R. (Eds.), Encyclopedia of Geology. Elsevier, Amsterdam, pp. 217–233.

Bell, K., Simonetti, A., 2010. Source of parental melts to carbonatites–critical isotopic constraints. Mineralogy and Petrology 98, 77–89.

Bell, K., Blenkinsop, J., Cole, T.J.S., Menagh, D.P., 1982. Carbonatites: genesis and evolution. Nature 298, 251–253.

Bell, K., Zaitsev, A.N., Spratt, J., Fröjdö, S., Rukhlov, A.S., 2015. Elemental, lead and sulfur isotopic compositions of galena from Kola carbonatites, Russia–implications for melt and mantle evolution. Mineralogical Magazine 79, 219–241.

Brigatti, M.F., Medici, L., Saccani, E., Vaccaro, C., 1996. Crystal chemistry and petrologic significance of Fe^{3+}–rich phlogopite from the Tapira carbonatite complex, Brazil. American Mineralogist 81, 913–927.

Brod, J.A., Gaspar, J.C., Araújo, D.P., Gibson, S.A., Thompson, R.N., Junqueira–Brod, T.C., 2001. Phlogopite and tetra-ferriphlogopite from Brazilian carbonatite complexes: petrogenetic constraints and implications for mineral chemistry systematics. Journal of Asian Earth Sciences 19, 265–296.

Chakhmouradian, A.R., 2006. High-field-strength elements in carbonatitic rocks: geochemistry, crystal chemistry and significance for constraining the sources of carbonatites. Chemical Geology 235, 138–160.

Chakhmouradian, A.R., 2009. The geochemistry of carbonatites revisited: two major types of continental carbonatites and their trace-element signatures. Geophysical Research Abstracts 11 (EGU2009-10806).

Chakhmouradian, A.R., Mumin, A.H., Demény, A., Elliott, B., 2008. Postorogenic carbonatites as Eden Lake Trans–Hudson orogen (northern Manitoba, Canada): geological setting, mineralogy and geochemistry. Lithos 103, 503–526.

Chen, J.F., Xie, A., Li, H.M., Zhang, X.D., Zhou, T.X., Park, Y.S., Ahn, K.S., Chen, D.G., Zhang, X., 2003. U–Pb zircon ages for a collision-related K-rich complex at Shidao in the Sulu ultrahigh pressure terrane, China. Geochemical Journal 37, 35–46.

Choi, S.G., Cho, J.M., Kim, D.W., Seo, J., Park, J.W., Kim, N.W., 2013. Geochemical and mineralogical characteristics of the Yonghwa phoscorite–carbonatite complex, Korea. 12th Biennial SGA Meeting. Mineral Deposit Research for a High–Tech World. Proceedings 3, Uppsala Sweden, pp. 1702–1704.

Choi, S.G., Rajesh, V.J., Seo, J., Park, J.W., Oh, C.W., Pak, S.J., Kim, S.W., 2009. Petrology, geochronology and tectonic implications of Mesozoic high Ba–Sr granites in the Haemi area, Hongseong Belt, South Korea. Island Arc 18, 266–281.

Cooper, A.F., Reid, D.L., 1998. Nepheline sövites as parental magmas in carbonatite complexes: evidence from Dicker Willem, Southwest Namibia. Journal of Petrology 39, 2123–2136.
Cordeiro, P.F.O., Brod, J.A., Dantas, E.L., Barbosa, E.S.R., 2010. Mineral chemistry, isotope geochemistry and petrogenesis of niobium-rich rocks form the Catalão carbonatite–phoscorite complex, Central Brazil. Lithos 118, 223–237.
Deines, P., 1989. Stable isotope variations in carbonatites. In: Bell, K. (Ed.), Carbonatites: Genesis and Evolution. Unwin Hyman, London, pp. 301–359.
Demény, A., Ahijado, A., Casillas, R., Vennemann, T.W., 1998. Crustal contamination and fluid/rock interaction in the carbonatites of Fuerteventura (Canary Island, Spain): a C, O, H isotope study. Lithos 44, 101–105.
Dewey, J.F., 1988. Extensional collapse of orogens. Tectonics 7, 1123–1139.
Dixey, F., Smith, W.C., Bisset, C.B., 1935. The Chilwa Series of Southern Nyasaland: Geological Survey. Nyasaland Bulletin 5 p. 82 (Revised, 1995).
Downes, H., Balaganskaya, E., Beard, A., Liferovich, R., Demaiffe, D., 2005. Petrogenetic processes in the ultramafic, alkaline and carbonatitic magmatism in the Kola Alkaline Province: a review. Lithos 85, 48–75.
Drüppel, K., Hoefs, J., Okrusch, M., 2005. Fenitizing processes induced by ferrocarbonatite magmatism at Swartbooisdrif, NW Namibia. Journal of Petrology 46, 377–406.
Drüppel, K., Wagner, T., Boyce, A., 2006. Evolution of sulfide mineralization in ferrocarbonatite, Swartbooisdrif, northwestern Namibia: constraints from mineral compositions and sulfur isotopes. Canadian Mineralogist 44, 877–894.
Farrell, S., Bell, K., Clark, I., 2010. Sulphur isotopes in carbonatites and associated silicate rocks from the Superior Province, Canada. Mineralogy and Petrology 98, 209–226.
Faure, G., 2001. Origin of Igneous Rocks; the Isotopic Evidence. Springer–Verlag, Heidelberg.
Faure, G., Mensing, T.M., 2005. Isotopes: Principles and Applications. 3rd edition. Wiley (928 pp.).
Gieré, R., 1996. Formation of rare earth minerals in hydrothermal systems. In: Jones, A.P., Wall, F., Williams, C.T. (Eds.), Rare Earth Minerals: Chemistry, Origin and Ore Deposits. Chapman and Hole, pp. 105–150.
Gittins, J., 1989. The origin and evolution of carbonatite magmas. In: Bell, K. (Ed.), Carbonatites: Genesis and Evolution. Unwin Hyman, London, pp. 580–600.
Gittins, J., Harmer, R.E., 1997. What is ferrocarbonatite? A revised classification. Journal of African Earth Sciences 25, 159–168.
Gittins, J., Allen, C.R., Cooper, A.F., 1975. Phlogopitization of pyroxenite; its bearing on the composition of carbonatite magmas. Geological Magazine 112, 503–507.
Gomide, C.S., Brod, J.A., Junqueira–Brod, T.C., Buhn, B.M., Santos, R.V., Barbosa, E.S.R., Cordeiro, P.F.O., Palmieri, M., Grasso, C.B., Torres, M.G., 2013. Sulfur isotopes from Brazilian alkaline carbonatite complexes. Chemical Geology 341, 38–49.
Guo, Z., Wilson, M., Liu, J., Mao, Q., 2006. Post–collisional, potassic and ultrapotassic magmatism of the northern Tibetan plateau: constraints on characteristics of the mantle source, geodynamic setting and uplift mechanisms. Journal of Petrology 47, 1177–1220.
Harmer, R.E., 1999. The petrogenetic association of carbomatite and alkaline magmatism: constraints from the Spitskop complex, South Africa. Journal of Petrology 40, 525–548.
Hawthorne, F.C., Oberti, R., Harlow, G.E., Maresch, W.V., Martin, R.F., Schumacher, J.C., Welch, M.D., 2012. IMA report: nomenclature of the amphibole supergroup. American Mineralogist 97, 2031–2048.
Heathcote, R.C., McCormick, G.R., 1989. Major-cation substitution in phlogopite and evolution of carbonatite in the Potash Sulfur Springs complex, Garland County, Arkansas. American Mineralogist 74, 132–140.
Heinrich, E.W., 1966. The Geology of Carbonatites. Rand McNally, Chicago.
Heinrich, E.W., 1967. Carbonatites: nil–silicate igneous rocks. Earth Science Reviews 3, 203–210.
Hoefs, J., Nielsen, H., Schidlowski, M., 1968. Sulphur isotope abundances in pyrite from the Witwatersrand conglomerates. Economic Geology 63, 975–977.
Hogarth, D.D., 1989. Pyrochlore, apatite and amphibole: distinctive minerals in carbonatite. In: Bell, K. (Ed.), Carbonatites: Genesis and Evolution. Unwin Hyman, London, pp. 105–148.
Hou, Z.Q., Tian, S., Yuan, Z., Xie, Y., 2006. The Himalayan collision zone carbonatites in western Sichuan, SW China: petrogenesis, mantle source and tectonic implication. Earth and Planetary Science Letters 244, 234–250.
Jeong, Y.J., Yi, K., Kamo, S.L., Cheong, C.S., 2008. ID–TIMS single zircon age determination of mangerite in the eastern Gyeonggi Massif, Korea. Journal of the Geological Society of Korea 44, 425–433.
Karchevsky, P.I., Moutte, J., 2004. The phoscorite–carbonatite complex of Vuoriyarvi, northern Karelia. In: Wall, F., Zaitsev, A.N. (Eds.), Phoscorites and Carbonatites from Mantle to Mine: the Key Example of the Kola Alkaline Province. Mineralogical Society Series 10, pp. 163–169 (London).
Keller, J., Hoefs, J., 1995. Stable isotope characteristic of recent natrocarbonatites from Oldoinyo Lengai. In: Bell, K., Keller, J. (Eds.), Carbonatite Volcanism: Oldoinyo Lengai and the Petrogenesis of Natrocarbonatites. Springer, Berlin, pp. 113–123.
Kim, N., Cheong, C.S., Yi, K., Jeong, Y.J., Koh, S.M., 2016. Post-collisional carbonatite-hosted rare earth element mineralization in the Hongcheon area, central Gyeonggi massif, Korea: ion microprobe monazite U–Th–Pb geochronology and Nd–Sr isotope geochemistry. Ore Geology Reviews 79, 78–87.
Kim, S.W., Kwon, S., Koh, H.J., Yi, K., Jeong, Y.J., Santosh, M., 2011. Geotectonic framework of Permo–Triassic magmatism within the Korean Peninsula. Gondwana Research 20, 865–889.
Krasnova, N.I., Balaganskaya, E.G., Garcia, D., 2004. Kovodr — classic phoscorites and carbonatites. In: Wall, F., Zaitsev, A.N. (Eds.), Phoscorites and Carbonatites from Mantle to Mine: the Key Example of the Kola Alkaline Province. Mineralogical Society Series 10. The Mineralogical Society of Great Britain & Ireland, London, pp. 99–132.
Kresten, P., 1988. The chemistry of fenitization: exsamples from Fen, Norway. Chemical Geology 68, 329–349.
Le Bas, M.J., 1977. Carbonatite–Nephelinite Volcanism: An Africa Case History. Wiley, London.
Le Bas, M.J., 1999. Ferrocarbonatites: geochemistry and magma–fluid state. Memoirs of the Geological Society of India 43, 785–802.
Le Bas, M.J., 2008. Fenites associated with carbonatites. Canadian Mineralogist 46, 915–932.
Le Maitre, R.W., 2002. Igneous Rocks: A Classification and Glossary of Terms. 2nd editions. Cambridge University Press (236 pp.).
Lee, M.J., Garcia, D., Moutte, J., Lee, J.I., 2003. Phlogopite and tetraferriphlogopite from phoscorite and carbonatite associations in the Sokli massif, northern Finland. Geosciences Journal 7, 9–20.
Lee, M.J., Garcia, D., Moutte, J., Williams, C.T., Wall, F., 2004. Carbonatites and phoscorites from the Sokli Complex, Finland. In: Wall, F., Zaitsev, A.N. (Eds.), Phoscorites and Carbonatites from Mantle to Mine: The Key Example of the Kola Alkaline Province. Mineralogical Society Series 10. The Mineralogical Society of Great Britain & Ireland, London, pp. 133–162.
Mäkelä, M., Vartiainen, H., 1978. A study of sulfur isotopes in the Sokli multi–stage carbonatite (Finland). Chemical Geology 21, 257–265.
Mariano, A.N., 1989. Nature of economic mineralization in carbonatites and related rocks. In: Bell, K. (Ed.), Carbonatites: Genesis and Evolution. Unwin Hyman, London, pp. 149–176.
McDonough, W.F., Sun, S.S., 1995. The composition of the earth. Chemical Geology 120, 223–253.
Melgarejo, J.C., Costanzo, A., Bambi, A.C.J.M., Goncalves, A.O., Neto, A.B., 2012. Subsolidus processes as a key factor on the distribution of Nb species in plutonic carbonatites: the Tchivira case, Angola. Lithos 152, 187–201.
Mitchell, R.H., 2005. Carbonatites and carbonatites and carbonatites. Canadian Mineralogist 43, 2049–2068.
Mitchell, R.H., 2015. Primary and secondary niobium mineral deposits associated with carbonatites. Ore Geology Reviews 64, 626–641.
Mitchell, R.H., Krouse, H.R., 1975. Sulphur isotope geochemistry of carbonatites. Geochimica et Cosmochimica Acta 39, 1505–1513.
Morbidelli, L., Gomes, C.B., Beccaluva, L., Brotzu, P., Conte, A.M., Ruberti, E., Traversa, G., 1995. Mineralogical, petrological and geochemical aspects of alkaline and alkaline–carbonatite associations from Brazil. Earth-Science Reviews 39, 135–168.
Nelson, D.R., Chivas, A.R., Chappell, B.W., McCulloch, M.T., 1988. Geochemical and isotopic systematics in carbonatites and implications for the evolution of ocean–island sources. Geochimica et Cosmochimica Acta 52, 1–7.
Nielsen, H., 1979. Sulfur isotopes. In: Jäger, E., Hunziker, H.C. (Eds.), Lectures in Isotope Geology. Springer–Verlag, Heidelberg, pp. 283–312.
Oh, C.W., Kusky, T.M., 2007. The Late Permian to Triassic Hongseong–Odaesan collision belt in South Korea, and its tectonic correlation with China and Japan. International Geology Review 49, 636–657.
Oh, C.W., Kim, S.W., Choi, S.G., Zhai, M., Guo, J., Sajeev, K., 2005. First finding of eclogite facies metamorphic event in South Korea and its correlation with the Dabie–Sulu collision belt in China. Journal of Geology 113, 226–232.
Oh, C.W., Krishnan, S., Kim, S.W., Kwon, Y.W., 2006. Mangerite magmatism associated with a probable Late-Permian to Triassic Hongseong–Odaesan collision belt in South Korea. Gondwana Research 9, 95–105.
Ohmoto, H., 1972. Systematics of Sulphur and carbon isotopes in hydrothermal ore deposits. Economic Geology 67, 551–578.
Ohmoto, H., Rye, R.O., 1979. Isotopes of sulfur and carbon. In: Barnes, H.L. (Ed.), Geochemistry of Hydrothermal Ore Deposits, 2nd editions Wiley and Sons, New York, pp. 509–567.
Peccerillo, R., Taylor, S.R., 1976. Geochemistry of Eocene calc–alkaline volcanic rocks from the Kastamonu area, northern Turkey. Contributions to Mineralogy and Petrology 58, 63–81.
Peng, P., Zhai, M., Guo, J., Zhang, H., Zhang, Y., 2008. Petrogenesis of Triassic postcollisional syenite plutons in the Sino-Korean craton: an example from North Korea. Geological Magazine 145, 637–647.
Platt, R.G., Woolley, A.G., 1990. The carbonatites and fenite of Chipman Lake, Ontario. Canadian Mineralogist 28, 241–250.
Ribeiro, C.C., Brod, J.A., Junqueira–Brod, T.C., Gaspar, J.C., Petrinovic, I.A., 2005. Mineralogical and field aspects of magma fragmentation deposits in a carbonate–phosphate magma chamber: evidence from the Catalão I complex, Brazil. South American Earth Sciences 18, 355–369.
Ripley, E.M., 1999. Systematics of S and O isotopes in mafic igneous rocks and related Cu–Ni–PGE mineralization. In: Keays, R.R., Lesher, C.M., Lightfoot, P.C., Farrow, C.E.G. (Eds.), Dynamic Processes in Magmatic Ore Deposits and their Application to Mineral ExplorationGeological Association of Canada Short Course 13. Geological Association of Canada, Newfoundland, Canada, pp. 133–158.
Rollinson, H., 1993. Using Geochemical Data: Evaluation, Presentation, Interpretation. Addison Wesley Longman, Essex, UK (352 pp.).
Russell, D.H., Heimstra, S.A., Groeneveld, D., 1954. The mineralogy and petrology of the carbonatite at Loolekop, eastern Transvaal. Transactions Geological Society of South Africa 57, 197–208.
Ryabchikov, I.D., Kogarko, L.N., Krivdik, S.G., Ntaflos, T., 2008. Constraints of the formation of carbonatites in the Chernigovka massif, Azov region, Ukraine. Geology of Ore Deposits 50, 423–432.
Sagong, H., Kwon, S.T., 2005. Mesozoic episodic magmatism in South Korea and its tectonic implication. Tectonics 24, 1–18.
Sakai, H., 1968. Isotopic properties of sulfur compounds in hydrothermal processes. Geochemical Journal 2, 29–49.
Santos, R.V., Clayton, R.N., 1995. Variations of oxygen and carbon isotopes in carbonatites: a study of Brazilian alkaline complexes. Geochimica et Cosmochimica Acta 59, 1339–1352.

Seo, J., Choi, S.G., Oh, C.W., 2010. Petrology, geochemistry, and geochronology of the post-collisional Triassic mangerite and syenite in the Gwangcheon area, Hongseong Belt, South Korea. Gondwana Research 18, 479–496.
Sharygin, V.V., Sobolev, N.V., Channer, D.M.D.R., 2009. Oscillatory-zoned crystals of pyrochlore — group minerals from the Guaniamo kimberlites, Venezuela. Lithos 112S, 976–985.
Sharygin, V.V., Zhitova, L.M., Nigmatulina, E.N., 2011. Fairchildite $K_2Ca(CO_3)_2$ in phoscorites from Phalaborwa, South Africa: the first occurrence in alkaline carbonatite complexes. Russian Geology and Geophysics 52, 208–219.
Sun, S.S., McDonough, W.F., 1989. Chemical and isotopic systematic of oceanic basalt: implications for mantle composition and process. In: Saunders, A.D., Norry, M.J. (Eds.), Magmatism in the Ocean Basins. Geological Society of London, Special Publication vol. 42, pp. 528–548.
Taylor Jr., H.P., J., F., Degens, E.T., 1967. Oxygen and carbon isotope studied of carbonatites from the Laacher See District, West Germany and the Alno District, Sweden. Geochimica et Cosmochimica Acta 31, 407–430.
Tilton, G.R., Bryce, J.G., Mateen, A., 1998. Pb–Sr–Nd isotope data from 30 and 300 Ma collision zone carbonatites in Northwest Pakistan. Journal of Petrology 39, 1865–1874.
Veksler, I.V., Nielsen, T.F.D., Sokolov, S.V., 1998. Mineralogy of crystallized melt inclusions from Gardiner and Kovdor ultramafic alkaline complexes: implications for carbonatite genesis. Journal of Petrology 39, 2015–2031.
Verwoerd, W.J., 1966. South African Carbonatites and Their Probable Mode of Origin. Ann. Univ. Stellenbosch Ser. A 41 p. 233.
Von Gehlen, K., 1967. Sulfur isotopes from the sulphide bearing carbonatite of Phalabora, South Africa. Transactions of the Institution of Mining and Metallurgy 76B (abstract).
Von Gehlen, K., 1992. Sulfur in the earth's mantle — a review. In: Schidlowski, M., Golubic, S., Kimberley, M.M., McKirdy, D.M., Trudinger, P.A. (Eds.), Early Organic Evolution: Implications for Mineral and Energy Resources. Springer, Berlin Heidelberg, pp. 359–366.
Williams, I.S., Cho, D.L., Kim, S.W., 2009. Geochronology, and geochemical and Nd–Sr isotopic characteristics, of Triassic plutonic rocks in the Gyeonggi Massif, South Korea: constraints on Triassic post-collisional magmatism. Lithos 107, 239–256.
Woolley, A.R., 2001. Alkaline Rocks and Carbonatites of the World. (Part 3). The Geological Society, London (384 pp.).
Woolley, A.R., Church, A.A., 2005. Extrusive carbonatites: a brief review. Lithos 85, 1–14.
Woolley, A.R., Kempe, D.R.C., 1989. Carbonatites: nomenclature, average chemical compositions, and element distribution. In: Bell, K. (Ed.), Carbonatites: Genesis and Evolution. Unwin Hyman, London, pp. 1–14.
Woolley, A.R., Kjarsgaard, B.A., 2008. Paragenetic types of carbonatite as indicated by the diversity and relative abundances of associated silicate rock: evidence from a global database. Canadian Mineralogist 46, 741–752.
Xu, C., Taylot, R.N., Kynicky, J., Chakhmouradian, A.R., Song, W., Wang, L., 2011. The origin of enriched mantle benesth North China block: evidence from young carbonatites. Lithos 127, 1–9.
Yang, J.H., Chung, S.L., Wilde, S.A., Wu, F.Y., Chu, M.F., Lo, C.H., Fan, H.R., 2005. Petrogenesis of post–orogenic syenites in the Sulu Orogenic Belt, East China: geochronological, geochemical and Nd–Sr isotopic evidence. Chemical Geology 214, 99–125.
Yegorov, L.S., 1993. Phoscorites of the Maymecha–Kotuy ijolite–carbonatite association. International Geology Review 35, 346–358.